PERGAMON

Chemosphere 42 (2001) 571–577

CHEMOSPHERE

Kinetic studies of the reaction of hydroxyl radicals with trichloroethylene and tetrachloroethylene

LeAnn B. Tichenor [a], Abdulaziz El-Sinawi [a], Takahiro Yamada [a], Philip H. Taylor [a,*], Jingping Peng [b], Xiaohua Hu [b], Paul Marshall [b]

[a] *Environmental Sciences and Engineering Group, University of Dayton Research Institute, 300 College Park, Dayton, OH 43469-0132, USA*

[b] *Department of Chemistry, University of North Texas, P.O. Box 305070, Denton, TX 76203-5070, USA*

Abstract

Rate coefficients are reported for the gas-phase reaction of the hydroxyl radical (OH) with C_2HCl_3 (k_1) and C_2Cl_4 (k_2) over an extended temperature range at 740±10 Torr in a He bath gas. These absolute rate measurements were accomplished using a laser photolysis/laser-induced fluorescence (LP/LIF) technique under slow flow conditions. The simple Arrhenius equation adequately describes the low temperature data for k_1 (<650 K) and the entire data set for k_2 and is given by (in units of cm^3 $molecule^{-1}$ s^{-1}):

$$k_1(291-650\ \mathrm{K}) = (9.73 \pm 1.15) \times 10^{-13} \exp(158.7 \pm 44.0)/T,$$

$$k_2(293-720\ \mathrm{K}) = (1.53 \pm 0.14) \times 10^{-12} \exp(-688.2 \pm 67.5)/T.$$

Error limits are 2σ values. The room temperature values for k_1 and k_2 are within $\pm 2\sigma$ of previous data using different techniques. The Arrhenius activation energies for k_1 and k_2 are a factor of 2–3 lower than previously reported values. The experimental measurements for both k_1 and k_2 in conjunction with transition state and variation transition state theory calculations infer an OH addition mechanism. The lack of a measurable kinetic isotope effect for k_1 is consistent with this mechanism. Insight into the subsequent reactions of the chemically activated intermediate are presented in the form of potential energy diagrams derived from ab initio calculations.

Keywords: Chlorinated hydrocarbons; Hydroxyl; Kinetics; Oxidation, reaction mechanisms

1. Introduction

Past and present manufacturing and disposal practices have resulted in the release of trichloroethylene (C_2HCl_3) and tetrachloroethylene (C_2Cl_4) into the atmosphere at significant rates. The annual amount of C_2HCl_3 and C_2Cl_4 emitted in the US alone was estimated to be $\sim 2.5 \times 10^5$ and $\sim 1 \times 10^5$ metric tons, respectively (Gilbert et al., 1980; Thomas et al., 1981).

The dominant atmospheric loss reaction is reaction with OH radicals since chloroethenes do not absorb radiation at wavelengths >300 nm, nor do they react significantly with O_3 or NO_3 in the gas phase (Atkinson et al., 1987; Atkinson, 1989). Rate constants at low temperatures (220–430 K) have been reported previously (Howard, 1976; Chang and Kaufman, 1977; Davis et al., 1977; Kirchner et al., 1990). The reaction mechanism is presumed to be addition to the π electrons associated with the C=C double bond. Kirchner et al. (1990), measured reaction products from OH reactions with C_2HCl_3 and C_2Cl_4 at low temperatures (300–450 K) using electron impact mass spectrometry. The observed

* Corresponding author. Fax: +1-937-229-2503.
E-mail address: taylorph@udri.udayton.edu (P.H. Taylor).

0045-6535/01/$ - see front matter
PII: S0045-6535(00)00229-0

product distributions were complex with the dominant mass spectra signals interpreted in terms of a reaction mechanism involving OH addition and subsequent Cl elimination. The relative importance of adduct stabilization versus Cl elimination has not been determined.

High temperature incineration is considered to be the best available technology for the safe disposal of these toxic compounds. The fastest process contributing to the destruction of halogenated hydrocarbons is the reaction with OH radicals (Fairchild et al., 1982; Warnatz et al., 1982). Given the lack of available data above 400 K, knowledge of the reaction rate constants and reaction mechanisms over an extended temperature range is essential to accurately predict the combustion behavior of these compounds.

We present atmospheric pressure, absolute rate coefficients for the reaction of OH with C_2HCl_3 (and C_2DCl_3) (k_1) and C_2Cl_4 (k_2) over an extended temperature range:

$$C_2HCl_3 + \bullet OH \rightarrow \text{products} \quad (k_1)$$
$$C_2Cl_4 + \bullet OH \rightarrow \text{products} \quad (k_2)$$

Arrhenius parameters are derived from the data. A comparison of these measurements with prior measurements at lower temperatures and pressures is discussed. Insight into the possible reaction mechanisms is also discussed based on transition state theory and variational transition state theory calculations and ab initio calculations of plausible reaction channels.

2. Experimental approach and data reduction

The experimental procedures were similar to those used in previous studies of the reaction of OH radicals with halogenated hydrocarbons (Fang et al., 1997, 1999). The method used to generate the precursor for the hydroxyl radical varied from previous experimentation. Initial testing of C_2HCl_3 and C_2Cl_4 was performed using 193 nm photolysis of N_2O/H_2O as the OH source, as had been done previously. The resulting room-temperature rate measurements exceeded previously reported values by a factor of two (C_2HCl_3) and 10 (C_2Cl_4) (Howard, 1976; Chang and Kaufman, 1977; Davis et al., 1977; Kirchner et al., 1990). Due to the large absorption cross-sections of C_2HCl_3 and C_2Cl_4 ($>5\times10^{-18}$ cm^2/molecule) (Zabel, 1974), additional measurements were conducted at low excimer laser fluences (<1 mJ cm^{-2}), with no observed reduction in rate coefficients. These results indicated that operation at 193 nm was unacceptable and necessitated the use of a different OH generation method. To minimize substrate photolysis, HONO was used as a hydroxyl radical source, which dissociated to NO and OH when exposed to near-UV radiation of 351 nm. A XeF excimer laser (Lamba Physik Compex Model 102) was used as the photodissociation source. Initial $[OH]_0$ ranged from ~ 2 to 4×10^{11} molecules cm^{-3}, and was determined based on the measured excimer fluence (9–18 mJ cm^{-2}), the published value of the absorption cross-section for HONO, 2.12×10^{-19} cm^2/ molecule at 351 nm (Demore et al., 1997), a quantum yield of 1.0 (Cox, 1974), and measured values of $[NO_2^-]$ taken to represent [HONO] determined using ion chromatography ($\sim 5\times10^{13}$ molecules cm^{-3}).

Initial substrate concentrations ranged from $\sim 3\times10^{13}$ to 1×10^{15} molecules cm^{-3}. All experiments were conducted at a total pressure of 740 ± 10 Torr. Samples of C_2HCl_3 and C_2Cl_4 were obtained from Aldrich with 99.9% purity. Gas chromatography-mass spectrometry (GC/MS) analyses indicated that this purity was met or exceeded.

Initial measurements at or near room temperature required passivation of the injector probe prior to collecting reliable data. Following these measurements, the injection probe was cleaned and treated with boric acid to reduce the reactivity of the surface. Subsequent measurements taken over a three month time period did not show any re-occurring effects of surface adsorption.

The rate of disappearance of the OH may be presented as:

$$-\mathrm{d}[OH]/\mathrm{d}t = k[A_o][OH] + k_d[OH]$$

where k is the bimolecular rate constant, A_o the organic concentration, and k_d is the first-order rate for the reaction of OH with impurities; considers diffusion out of the reaction volume.

This relationship holds in the absence of any secondary reactions that may form or deplete OH. Solution of this equation yields $[OH] = [OH]_o \exp(-k't)$, where $k' = k + k_d$. For all experiments, reactive and diffusive OH radical decay profiles exhibited exponential behavior and were fitted by the following nonlinear expression:

$$[OH] = [OH]_o \exp(-k't) + \gamma,$$

where γ is the constant background signal level and t is the time delay between the laser pulses. As the organic concentration was much greater than the [OH], pseudo first-order exponential OH decays were observed and the individual temperature dependent rate constants were determined by $k' = k[\text{organic}] + k_d$, where the bimolecular rate constant k, is the slope of the least-squares fit of k′ versus the [organic]. OH decays were observed over two to three decay lifetimes over a time interval of 0.3–20.0 ms.

3. Results

Absolute rate coefficients for k_1 and k_2 are presented in Tables 1 and 2, respectively. Random error limits

($\pm 2\sigma$) were below 20% in most cases. When identifying possible side reactions, two reactions of concern are hydroxyl and/or organic reaction with excess HCl and H_2O. These two compounds were present in the system as carryovers from the HONO reactor. These and other possible side reactions were simulated numerically using reaction rate constants published in the NIST chemical kinetics database (Mallard, 1998). The results of this analysis indicated that side reactions would not impact significantly on the reaction under observation with the input concentrations used. In the absence of reactant impurities, sources of systematic error were then limited to thermally-induced secondary reactions. The possibility of thermally-induced side products was investigated by varying the total gas flow rate. k_1 and k_2 was found to be independent of the residence time in the mid to high-temperature regions, implying a lack of thermal reaction of the substrates at elevated temperatures. Above 750 K, an excess of OH radical generation in the absence of the photolytic laser pulse was observed, and OH decays were not measurable.

All known absolute rate measurements for k_1 and k_2 are summarized in Figs. 1 and 2, respectively. This work extends experimental measurement beyond the limit of ~450 K reported previously. A variety of techniques were used in collecting these data. Examination of Figs. 1 and 2 shows agreement at room temperature, within combined experimental uncertainties, between our work and that reported previously (Howard, 1976; Chang and Kaufman, 1977; Davis et al., 1977; Kirchner et al., 1990).

Table 1
Absolute rate coefficients for k_1[a]

Temp (K)	10^{12} k_1 (cm^3 molecule^{-1} s^{-1})
291	1.81 ± 0.26
292	1.89 ± 0.24
292	1.72 ± 0.32[b]
293	1.70 ± 0.28
294	1.55 ± 0.22
326	1.56 ± 0.14
330	1.50 ± 0.18
356	1.44 ± 0.22
410	1.40 ± 0.20
417	1.41 ± 0.22
422	1.38 ± 0.32
467	1.40 ± 0.10
500	1.37 ± 0.32
502	1.37 ± 0.32
505	1.23 ± 0.18
508	1.37 ± 0.32
562	1.22 ± 0.20
621	1.40 ± 0.22
650	1.28 ± 0.34
699	1.35 ± 0.30[b]
709	1.67 ± 0.12
711	2.02 ± 0.18
719	1.64 ± 0.26
720	1.68 ± 0.15
746	2.00 ± 0.54
750	1.63 ± 0.26
752	1.94 ± 0.28

[a] Errors represent $\pm 2\sigma$ and do not include the 5–10% uncertainty estimated for possible systematic errors.
[b] C_2DCl_3.

Table 2
Absolute rate coefficients for k_2[a]

Temp (K)	10^{13} k_2 (cm^3 molecule^{-1} s^{-1})
293	1.52 ± 0.17
350	2.13 ± 0.13
400	2.85 ± 0.21
440	3.12 ± 0.12
500	4.06 ± 0.04
550	4.61 ± 0.41
640	5.50 ± 0.24
700	5.63 ± 0.18
720	5.88 ± 0.55

[a] Errors represent $\pm 2\sigma$ and do not include the 5–10% uncertainty estimated for possible systematic errors.

Rate measurements for k_1 exhibited complex behavior with a negative temperature dependence at temperatures below 650 K and a positive temperature dependence at higher temperatures. The simple Arrhenius equation adequately describes the low temperature data for k_1 (<650 K) and the entire data set for k_2 and is given by (in units of cm^3 molecule^{-1}s^{-1}):

$$k_1(291-650\ \mathrm{K}) = (9.73 \pm 1.15) \times 10^{-13} \times \exp(158.7 \pm 44.0)/T,$$

$$k_2(293-720\ \mathrm{K}) = (1.53 \pm 0.14) \times 10^{-12} \times \exp(-688.2 \pm 67.5)/T.$$

Error limits are 2σ values. Additional measurements for k_1 at higher temperatures (>750 K) are required to provide a statistically valid Arrhenius expression for this temperature regime. Although our room temperature data for both k_1 and k_2 are in agreement with previous studies, the measured temperature dependence differs considerably with previous studies. For C_2HCl_3, the Arrhenius activation energy derived from our lower temperature data (−315 cal/mol) is considerably lower than the values of −885 and −478 cal/mol reported by Chang and Kaufman (1977) and Kirchner et al. (1990), respectively, over more limited temperature ranges. Surface adsorption effects, a well-known source of systematic error in discharge flow type kinetic measurements, may be the cause of the enhanced reactivity and larger negative temperature dependence of C_2HCl_3 at sub-ambient temperatures in the previous measurements (see Fig. 1). For C_2Cl_4, the temperature dependence of our measurements from 293 to 720 K yields an Arrhenius activation energy of ~1.4 kcal/mol. This contrasts

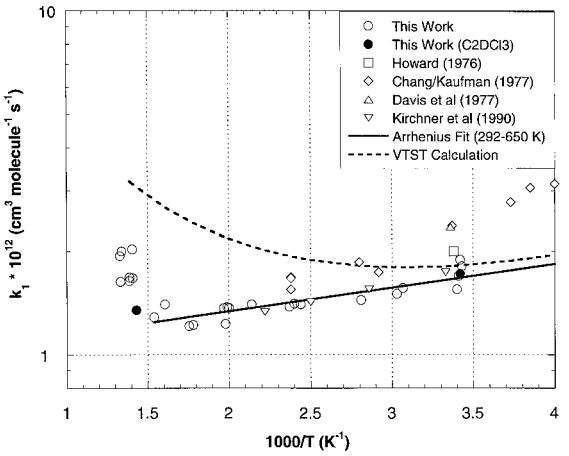

Fig. 1. Arrhenius plot of kinetic data for k_1. Also shown are the results of previous studies, an Arrhenius fit to the data from 291 to 650 K, and the results of variational transition state theory calculations ($P = 740 \pm 10$ Torr).

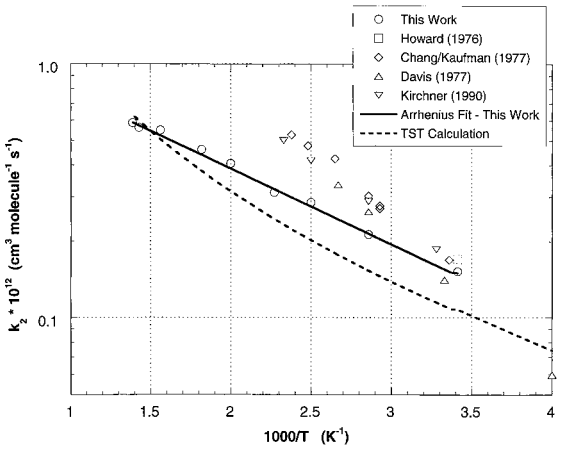

Fig. 2. Arrhenius plot of kinetic data for k_2. Also shown are the results of previous studies, an Arrhenius fit to the data, and the results of transition state theory calculations ($P = 740 \pm 10$ Torr).

with values of 2.4 and 2.0 kcal/mol reported by Chang and Kaufman (1977) and Kirchner, et al. (1990), respectively, over more limited temperature ranges. In this case, surface adsorption effects in the prior measurements, most prominent at lower temperatures, are inconsistent with the reduction in Arrhenius activation energy observed in our measurements. Previous studies have indicated that this reaction is not pressure dependent between 0.5 and 5.6 mbar (Kirchner et al., 1990). Theoretical calculations to be published elsewhere support the lack of a pressure dependence at these pressures (Tichenor et al., 1999). Therefore, the fact that the prior studies were performed at lower pressures (0.5–5.6 mbar) cannot explain the difference in reactivity. In the absence of reactant impurities, an explanation for the differences in reactivity for k_2 with increasing temperature currently elude us.

For k_1, rate coefficient measurements were also obtained with deuterated trichloroethylene to provide insight into the reaction mechanism. Rate coefficient measurements with C_2DCl_3 at 292 and 699 K indicate the absence of a measurable isotope effect (see Table 1). This result indicates that an OH addition mechanism dominates the measured OH decay rates throughout the temperature range of investigation. For k_2, an OH addition mechanism is also likely due to the large activation energy required for the Cl atom abstraction reaction ($\Delta H_{r\times n,298} = 28.7$ kcal/mol). [1]

[1] Geometries, frequencies, and ZPE calculated using B3LYP/6-31G(d). Total energy calculated using B3LYP/6-311+G(3df,2p).

3.1. Theoretical calculations

In addition to measured reaction rate expressions for k_1 and k_2, the reaction pathways and kinetics were analyzed using thermodynamic properties. Thermodynamic properties and kinetic parameters were determined for reactants, intermediate radicals, transition states (TSs), and products.

The potential energy diagram for k_1 is shown in Fig. 3(a) and (b) for OH radical attack at the α(CHCl) and β(CCl_2) site of the substrate. Literature values were used to estimate the $\Delta H^\circ_{f\ 298}$ of reactants (Stull and Prophet, 1971, Stull et al., 1987). GA method with THERM computer program (Ritter and Bozzelli, 1991) was used to calculate $\Delta H^\circ_{f\ 298}$ of intermediate radicals and products. Semi-empirical molecular orbital (MO) theory, PM3, with MOPAC6.0 computer code (Stewart, 1989), was performed to estimate E_as except entrance channel. E_as were estimated by taking energy difference between reactants (intermediate radicals) and TSs obtained by PM3 theory. $\Delta H^\circ_{f\ 298}$ derived by PM3 contains systematical errors, however, they effectively cancel when E_as are calculated by difference.

The potential energy diagram for k_2 is shown in Fig. 4. The energies were evaluated using a composite ab initio calculation, G3(MP2) (Curtiss et al., 1999) theory. Gaussian 94 and 98 computer codes were used to perform ab initio calculation on SGI-Origin2000 and Cray T-90 and 94 computers. The activation energy of TS0 (the entrance channel) was estimated using the higher-level G3 calculation (Curtiss et al., 1998) since this channel determines the OH decay rate and is the most critical of the reaction mechanisms. Energy calculations were estimated using the reactants as the basis for the

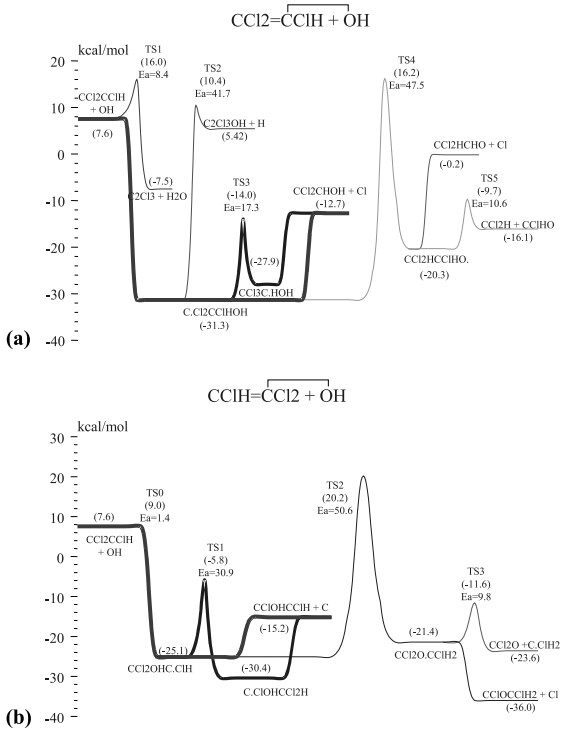

Fig. 3. (a) potential energy diagrams for the OH addition to C_2HCl_3 (α-site). Adduct stabilization, isomerization, H- and Cl-atom elimination channels are shown. Energies were evaluated using GA for the intermediate radicals and products and PM3 for E_a estimation. Thick lines represent energetically favorable pathways. (b) potential energy diagrams for the OH addition to C_2HCl_3 (β-site). Adduct stabilization, isomerization, H- and Cl-atom elimination channels are shown. Energies were evaluated using GA for the intermediate radicals and products and PM3 for E_a estimation. Thick lines represent energetically favorable pathways.

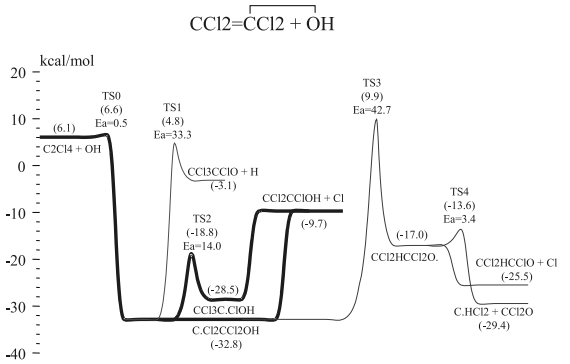

Fig. 4. Potential energy diagram for the OH addition to C_2Cl_4. Adduct stabilization, isomerization, H- and Cl-atom elimination channels are shown. Energies were evaluated using G3(MP2) theory except for TS1 (MP2(full)/g-31G(d)), TS2 (B3LYP/6–31G(d)), and the intermediate isomer $CCl_2HCCl_2O\bullet$(MP2(full)/g-31G(d)). E_a for TS1 was estimated by taking a difference between products and TS1 using MP2(full)/6–31G(d) level of theory because of convergence failure at the higher level of theory. E_a for TS2 was estimated using B3LYP/6–31G(d) level of theory because of optimization difficulty using MP2(full)/6–31G(d) level of theory and convergence failure at the higher level of theory. Thick lines represent energetically favorable pathways.

relative total energy difference. Zero point vibrational energy and thermal correction to 298 K were taken into account for the total energy calculation. Both G3 and G3(MP2) methods use HF/6–31G(d) level of theory to calculate frequencies and MP2(full)/6–31G(d) level of theory to optimize the geometry. G3 method then uses total energy calculated by QCISD(T)/6–31G(d), MP4/6–31G(d), MP4/6–31+G(d), MP4/6–31G(2df,p), and MP2(full)/G3large for the higher energy correction (Curtiss et al., 1998). G3(MP2) uses QCISD(T)/6–31G(d) and MP2(fc)/G3MP2large for the higher energy correction (Curtiss et al., 1999).

Variational transition state theory (VTST) calculations were performed to estimate the rate of OH addition to C_2HCl_3. In contrast to C_2Cl_4, conventional TST calculations are not useful because of the absence of a distinct barrier. The variational TST calculations were carried out as follows. First the reaction coordinate for addition of OH to the C = C bond was defined as a distinguished coordinate pathway (DCP) at the HF/6–31G(d,p) level. The geometry of the system was optimized at various fixed C–O separations, and frequencies were obtained normal to the DCP also at the HF/6–31G(d,p) level of theory. Then energies were computed at the spin-projected PMP4/6–311+G(d,p) level, relative to reactants. These energies, geometries, and frequencies were used to derive conventional TST rate constants as a function of position along the DCP. At each temperature, the VTST result was obtained by interpolation to find the minimum rate constant.

4. Discussion

The complex temperature dependence of k_1 is qualitatively consistent with VTST calculations of the entrance channel for the addition of OH to the H substituted side of the double bond of the substrate, which is based on PMP4/6–311+G(d,p) energies, the dominant site for addition (Kirchner et al., 1990). As illustrated in Fig. 1, these calculations exhibit a negative temperature dependence at low temperatures (<300 K) followed by a transition to a positive temperature dependence above ~500 K. The calculated transition state for the entrance channel is below the total energy of the reactants and is responsible for the negative temperature dependence at low temperatures. The transition to a positive

temperature dependence at higher temperatures is due to the increasing importance of the partition function that characterizes the transition state relative to the reactants. VTST calculations indicate that OH addition to the α site is the dominant reaction under the experimental conditions (Marshall et al., 2000). OH addition to the β site has a positive energy barrier and a factor of 8 lower A factor. This reaction increases in importance at very high temperatures (>2000 K). The lack of a measurable kinetic isotope effect is consistent with this analysis.

The positive temperature dependence of k_2 is consistent with the location of a transition state for OH addition to the π electron system that lies higher in energy than that of the reactants. This is in contrast to k_1 where the energy of the transition state (for OH addition to the α site) was below the energy of the reactants. Comparison of the measured rate coefficients with conventional TST calculations for the OH addition channel indicate generally good agreement, particularly at higher temperatures (see Fig. 2). The atypical large barrier for OH addition explains the metathesis-like behavior of the Arrhenius plot.

The potential energy surfaces shown in Figs. 3 and 4 provide some insight into the potential reaction mechanisms for k_1 and k_2, respectively. These surfaces indicate that both reactions are very likely chemically activated. Low energy Cl elimination pathways are available in both systems. The Cl elimination pathway is particularly facile for k_2, and may be expected to dominate from room temperature to temperatures characteristic of combustion systems. A H elimination channel may also contribute to the overall reaction at very high temperatures, in excess of 2000 K. The Cl elimination pathway is also favorable for k_1, but adduct stabilization is expected to be important at low temperatures due to the lack of an appreciable barrier to the formation of the activated complex. The lack of an experimentally observable H atom abstraction channel is consistent with the potential energy calculations for k_1 that indicate a substantial activation energy for this reaction.

Quantum RRK calculations based on the input parameters described in this manuscript are in progress and will be published in subsequent papers dealing with the kinetics and mechanism of reaction of OH with C_2HCl_3 and C_2Cl_4.

5. Conclusions

Rate coefficients are reported for the gas-phase reaction of the hydroxyl radical (OH) with C_2HCl_3 (k_1) and C_2Cl_4 (k_2) over an extended temperature range at 740 ± 10 Torr in a He bath gas. The room temperature values for k_1 and k_2 are within $\pm 2\sigma$ of previous data using different techniques. The temperature-dependent behavior of k_1 was observed to be complex, with the reaction exhibiting a slight negative activation energy below 650 K and a slight positive activation energy at higher temperatures (650–750 K). This contrasts with a factor of roughly 2–3 larger negative activation energy observed in previous lower temperature studies. The positive activation energy observed for k_2 (293–720 K) is about a factor of two lower than observed in previous lower temperature measurements. On the basis of potential energy surface calculations, reaction mechanisms involving Cl elimination are proposed to be important pathways in the oxidation of these compounds. H atom abstraction was not observed to be significant for k_1 under our experimental conditions, i.e., atmospheric pressure.

Acknowledgements

The authors acknowledge support from the Environmental Protection Agency (Grant R82-6169-01-0). The authors would also like to thank Dr. J.W. Bozzelli for his comments during the ab initio calculations. While this research has been supported by the US-EPA, it has not been subject to Agency review and therefore does not necessarily reflect the views of the Agency, and no official endorsement should be inferred.

References

Atkinson, R., 1989. J. Phys. Chem. Ref. Data, Monogr. 1.
Atkinson, R., Aschmann, S.M., Goodman, M.A., 1987. Int. J. Chem. Kinet. 19, 299.
Chang, J.S., Kaufman, F.J., 1977. Chem. Phys. 66, 4989.
Cox, R.A., 1974. J. Photochem. 3, 175.
Curtiss, L.A., Raghavachari, K., Redfern, P.C., Rassolov, V., Pople, J.A., 1998. J. Chem. Phys. 109, 7764.
Curtiss, L.A., Redfern, P.C., Raghavachari, K., Rassolov, V., Pople, J.A., 1999. J. Chem. Phys. 110, 4703.
Davis, D., Machado, U., Smith, G., Wagner, S., Watson, R.T., 1977. In: Watson, R.T., (Ed.), J. Phys. Chem. Ref. Data 6, p. 871, unpublished.
Demore, W.B., Goldent, D.M., Hampson, R.F., Kurylo, M.J., Howard, C.J., Ravishankara, A.R., Kolb, C.E., Molina, M.J. Jet Propulsion Laboratory Publ. 97-4, Chemical Kinetics and Photochemical Data for Use in Stratospheric Modeling, #12, National Aeronautics and Space Administration, 1997.
Fairchild, P.W., Smith, G.P., Crosley, D.R., 1982. In: Proceedings of the Nineteenth International Symposium on Combustion, The Combustion Institute, p. 107.
Fang, T.D., Taylor, P.H., Berry, R.J., 1999. J. Phys. Chem. A 103, 2700.
Fang, T.D., Taylor, P.H., Dellinger, B., Ehlers, C.J., Berry, R.J., 1997. J. Phys. Chem. 101, 5758.

Gilbert, D., Goyer, M., Lyman, W., Magil, G., Walker, P., Wallace, A., Wechsler, A., Yee, J. An exposure and risk assessment for tetrachloroethylene, EPA-440/4-85-015, 1980.

Howard, C.J., 1976. J. Chem. Phys. 65, 4771.

Kirchner, K., Helf, D., Ott, P., Vogt, S., 1990. Ber. Bunsenges. Phys. Chem. 94, 77.

Mallard, W.G., 1998. NIST Chemical kinetics database 2Q98, NIST standard reference database 17, US Department of Commerce, Gaithersburg, MD.

Marshall, P., Peng, J., Hu, X, El-Sinawi, A., Yamada, T., Taylor, P.H., In: proceeding 16th Int'l Symp. on Gas Kinetics, Cambridge, UK, July 2000.

Ritter, E.R., Bozzelli, J.W., 1991. J. Chem. Info. Comput. Sci. 31, 400.

Stewart, J.J.P., 1989. J. Comput. Chem. 10, 209.

Stull, D.R., Prophet, H., 1971. JANAF thermochemical tables second ed., US Department of Commerce, Gaithersburg, MD.

Stull, D.R., Westrum, J.E.F., Sinke, G., 1987. The Chemical Thermodynamics of Organic Compounds. Wiley, New York.

Thomas, R., Byrne, M., Gilbert, D., Goyer, M., Moss, K., 1981. An exposure and risk assessment for trichloroethylene, EPA-440/4-85-019.

Tichenor, L.B., Taylor, P.H., Yamada, T., Peng, J., Hu, X., Marshall, P., 1999. J. Phys. Chem. A, submitted.

Warnatz, J., Bockhorn, H., Moser, A., Wenz, H.W., 1982. In: Proceedings of the Nineteenth International Symposium on Combustion, The Combustion Institute, p. 197.

Zabel, F., 1974. Ber. Bunsenges. Phys. Chem. 78, 232.